特別掲載

Alpha-Ray Dosage near Thorotrast Aggregate

by

Yoshio Kato
Physics Division, National Institute of Radiological Sciences
Chiba, Japan

α 粒子によるトロトラスト顆粒近傍の吸収線量

放射線医学総合研究所　物理研究部
加　藤　義　雄

（昭和42年1月21日受付）

組織に吸着しているトロトラスト顆粒からの放射線による全放出エネルギーの約90％はα粒子によるといわれている．よつてこの顆粒から放出された大部分のエネルギーは顆粒のごく近くの組織に与えられることになり，その組織吸収線量は臓器全体の平均吸収線量よりはるかに大きな値になる．顆粒を球形と假定して，このα粒子による顆粒近傍の組織吸収線量ならびにこの顆粒の自己吸収を計算し，その結果を4例のトロトラスト患者の肝臓ならびに脾臓の組織標本の吸収線量推定に応用した．

Introduction

Thorotrast, a colloidal solution made of granules of thorium dioxide, was used during the period 1930–1945 as an outstanding agent of a contrast medium in angiography, hepatolienography and so on. After injection, thorotrast is taken up in the reticuloendothelial system, in which the granules of thorium dioxide remain indefinitely and form aggregates with dimension comparable to a range of α-particles emitted from the various members of the thorium decay chain. Radiations from the aggregates irradiate tissue for a long period of time, causing lesions. Thus thorotrast patients are interesting objects for the purpose of finding a relationship between the dosage and the lesion of tissue. Many workers[1-8] have searched for the absorbed dose averaged over a whole organ of the thorotrast patients. Rotblat et al.[3] and Rund[4] have showed that about 90 per cent of energy dissipated in tissue by the radiations emitted from the aggregates is carried by α-particles. Thus mot of the energy are dissipated in tissue within about 90μ (maximum range of the α-particles in tissue) from a surface of the thorotrast aggregates. This fact may justify that the dosage absorbed in tissue near the aggregate should be adopted as the dosage for a study of the dosage-lesion relationship, instead of the average dosage in the organ.

This paper describes an estimation of the dosage near the aggregate due to the α-partiles and that of an α-particle self-absorption in the aggregate as a function of an aggregate radius, and these results are also applied to an estimation of an average dose in some histological sections.

Absorbed dosage near the aggregate

In calculating the dosage, the form of the aggregate was assumed to be spherical in order to simplify a geometrical problem, and also the same assumptions as Spiers'[9)10)] were used : (1) the α-emitters are distributed uniformly in the aggregate, (2) the α-particles are emitted isotropically, (3) the α-particles travel in straight lines and have a constant linear energy transfer.

The absorbed dosage at a point, distance d from a surface of the aggregate, is given by

$$D(d) = \iiint \frac{N}{4\pi r^2} \cdot \frac{E}{R} \cdot r^2 \sin\theta d\phi dr d\theta, \tag{1}$$

where R is a range of the α-particle with an initial energy E in tissue, N a number of the α-particles emitted per unit volume of the aggregate and other parameters are shown in Fig. 1.

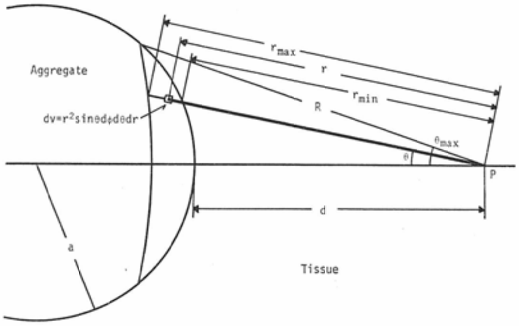

Fig. 1. The geometry used in calculating the energy dissipation near a surface of the spherical aggregate.

Integration of equation (1) with respect to ϕ and r gives

$$D(d) = \frac{NE}{2R} \cdot \int (r_{max} - r_{min}) \cdot \sin\theta d\theta = \frac{N \cdot E}{n} \cdot G, \tag{2}$$

where n is a ratio of the range of the α-particle in tissue to that in the aggregate, and G is a geometrical factor:

$$G = \frac{n}{2 \cdot R} \cdot \int (r_{max} - r_{min}) \cdot \sin\theta d\theta, \tag{3}$$

where an integrand and limits of the integration with respect to θ are as follows:

1) $\delta \geq \sqrt{1+\alpha^2} - \alpha$,

$$\frac{r_{max}-r_{min}}{R} = \frac{1}{n} \cdot \{1-(\alpha+\delta)\cos\theta + \sqrt{\alpha^2-(\alpha+\delta)^2\sin^2\theta}\}, \qquad 1 \geq \cos\theta \geq \frac{1+\delta^2+2\alpha\delta}{2(\alpha+\delta)},$$

2) $\sqrt{1+\alpha^2} - \alpha \geq \delta \geq 1-2n\alpha$,

(1) $$\frac{r_{max}-r_{min}}{R} = \frac{1}{n} \cdot \{1-(\alpha+\delta)\cos\theta + \sqrt{\alpha^2-(\alpha+\delta)^2\sin^2\theta}\}, \qquad 1 \geq \cos\theta \geq \cos\theta_s,$$

(2) $$\frac{r_{max}-r_{min}}{R} = 2\sqrt{\alpha^2-(\alpha+\delta)^2\sin^2\theta}, \qquad \cos\theta_s \geq \cos\theta \geq \frac{\sqrt{\delta^2+2\alpha\delta}}{\alpha+\delta},$$

$$\cos\theta_s = \frac{1}{4n(n-1)(\alpha+\delta)}\cdot\{(2n-1)\sqrt{1+4n(n-1)(\delta^2+2\alpha\delta)}-1\}, \tag{4}$$

3) $1-2n\alpha \geq \delta$,

$$\frac{r_{max}-r_{min}}{R} = 2\sqrt{\alpha^2-(\alpha+\delta)^2\sin^2\theta}, \qquad 1 \geq \cos\theta \geq \frac{\sqrt{\delta^2+2\alpha\delta}}{\alpha+\delta},$$

where $\alpha = a/R$ and $\delta = d/R$.

The integrating equation (3) with respect to θ gives the following expressions:

1) $\delta \geq \sqrt{1+\alpha^2}-\alpha$,

$$G = \frac{1}{2}\cdot\{1-\frac{\delta}{2}-\frac{1+\delta^2+2\alpha\delta}{4(\alpha+\delta)}+\frac{\delta^2+2\alpha\delta}{2(\alpha+\delta)}\cdot\log\delta\},$$

2) $\sqrt{1+\alpha^2}-\alpha \geq \delta \geq 1-2n\alpha$,

$$G = G_1 + G_2,$$

$$G_1 = \frac{1}{2}\cdot\{1-\frac{\delta}{2}-\frac{\cos\theta_s}{2}\cdot(2+\sqrt{\alpha^2-(\alpha+\delta)^2\sin^2\theta_s}-(\alpha+\delta)\cos\theta_s)$$

$$-\frac{\delta^2+2\alpha\delta}{2(\alpha+\delta)}\cdot\log(\frac{2\alpha+\delta}{(\alpha+\delta)\cos\theta_s+\sqrt{\alpha^2-(\alpha+\delta)^2\sin^2\theta_s}})\}, \tag{5}$$

$$G_2 = \frac{n}{2}\cdot\{\cos\theta_s\sqrt{\alpha^2-(\alpha+\delta)^2\sin^2\theta_s}-\frac{\delta^2+2\alpha\delta}{2(\alpha+\delta)}\cdot\log(\frac{\{(\alpha+\delta)\cos\theta_s+\sqrt{\alpha^2-(\alpha+\delta)^2\sin^2\theta_s}\}^2}{\delta^2+2\alpha\delta})\},$$

3) $1-2n\alpha \geq \delta$,

$$G = \frac{n}{2}\cdot\{\alpha-\frac{\delta^2+2\alpha\delta}{2(\alpha+\delta)}\cdot\log\frac{2\alpha+\delta}{\delta}\}.$$

α-particle self-absorption in the aggregate

According to the assumptions mentioned in the preceding section, the self-absorption, f, can be given by

$$f = \frac{n\cdot\overline{L}}{R}, \tag{6}$$

where $\overline{L}$ is a mean of the distance traversed in the aggregate:

$$\overline{L} = \frac{1}{\frac{4}{3}\pi a^3}\cdot\int_0^a\{\frac{1}{4\pi}\cdot\int_0^\pi\int_0^{2\pi}L\cdot\sin\theta' d\phi' d\theta'\}4\pi r^2 dr = \frac{3}{2a^3}\cdot\int_0^a\{\int_0^\pi L\cdot\sin\theta' d\theta'\}r^2 dr, \tag{7}$$

where L is given by

$$L = \begin{cases} r\cdot\cos\theta'+\sqrt{a^2-r^2\sin^2\theta'}, & \text{for } nL \leq R \\ R/n, & \text{for } nL > R \end{cases} \tag{8}$$

and other parameters are shown in Fig. 2.

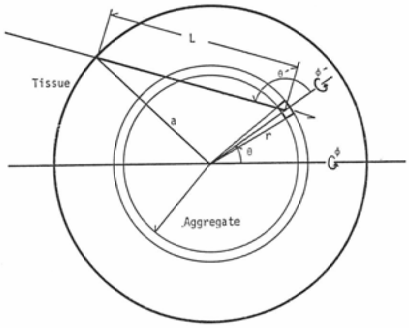

Fig. 2. The geometry used in calculating the self-absorption of the spherical aggregate.

The integrating of equation (7) with resepct to θ' and r gives

$$\overline{L} = \begin{cases} \frac{3}{4}\cdot a & \text{for } R \geq 2na, \\ \frac{R}{n} - \frac{3}{8}\cdot\frac{R^2}{an^2} + \frac{1}{64}\cdot\frac{R^4}{a^3n^4} & \text{for } R < 2na. \end{cases} \quad (9)$$

when equation (9) is substituted into equation (6), the self-absorption becomes

$$f = \begin{cases} \frac{3}{4}\cdot na & \text{for } R \geq 2na, \\ 1 - \frac{3}{8}\cdot\frac{1}{n\alpha} + \frac{1}{64n^3\alpha^3} & \text{for } R < 2na. \end{cases} \quad (10)$$

Dosage and self-absorption for the thorotrast aggregate

In the estimation of dosage and self-absotption, the values of the range of the α-particle in water, as shown in Fig. 3 and Table 1, were adopted as those in tissue, and the value of n is deduced from the Bragg-Kleeman rule[13], which gives the range in medium of atomic weight A and density ρ as follows:

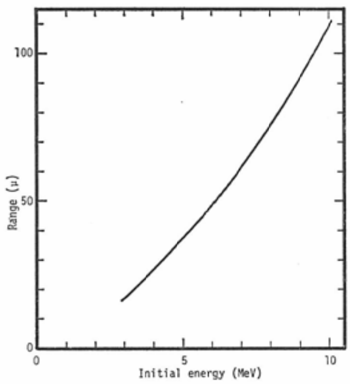

Fig. 3. The energy-range relationship of α-particle in water (Whaling[12]).

Table 1, Physical properties of the α-particles emitted from the members of the thorium decay chain.

Serial number	Nuclide	Decay constant*	α-particle energy*	Range** (in water)
		per year	MeV	μ
1	232-Th	0.495×10^{-10}	4.00	26.4
	228-Ra	0.103		
	228-Ac	0.990×10^{3}		
2	228-Th	0.363	5.39	42.0
3	224-Ra	0.695×10^{2}	5.66	44.5
4	220-Rn	0.424×10^{6}	6.28	52.4
5	216-Po	0.138×10^{9}	6.77	58.9
	212-Pb	0.573×10^{3}		
6	212-Bi	0.603×10^{4}	6.05 (0.36***)	49.5
7	212-Po	0.729×10^{14}	8.78 (0.64***)	88.6
	208-Tl	0.117×10^{6}		

* : Data from Strominger, Hollander and Seaborg[11]. ** : Data from Whaling[12].
*** : Branching ratio.

$$R = 3.2\text{x}10^{-4}\cdot\frac{\sqrt{A}}{\rho}\cdot R_{air}, \qquad \sqrt{A} = \frac{\sum_i n_i A_i}{\sum_i n_i\sqrt{A_i}}, \tag{11}$$

where R_{air} is the range in standard air and n_i is the atomic fraction of i-th element whose atomic weight is A_i. Then the value of n is deduced from equation (11) as follows:

$$n = \frac{R_{tissue}}{R_{ThO_2}} = \frac{\sqrt{A_{H_2O}}}{\sqrt{A_{ThO_2}}}\cdot\frac{\rho_{ThO_2}}{\rho_{H_2O}} = \frac{3.00}{11.4}\,\frac{9.87}{1.00} = 2.60.$$

When calculation was made of equations (5) and (10) by using the value drived for n and the value of R, the values of the geometrical factor as functions of α and δ became those as shown in Table 2 and were plotted in Fig. 4, and the value of the self-absorption as a function of α was plotted in Fig. 5.

Since thorium emits seven kinds of the α-particles, a dosage and a mean self -absorption vary with a degree of radioactive equilibirum state of the thorium decay chain in the aggregate. When an activity ratio of i-th α-emitting element to ^{232}Th is p_i, the dosage and the mean self-absorption are given by

$$D(d) = \frac{N}{n}\cdot\sum_i p_i E_i G_i = \frac{\rho N_0 \lambda}{nA}\cdot\sum_i p_i E_i G_i = 0.686\text{x}10^{4}\cdot\sum_i p_i E_i(\text{MeV})G_i \quad \text{in rad/year}, \tag{12}$$

and

$$\overline{f} = \frac{\sum_i p_i E_i f_i}{\sum_i p_i E_i}, \tag{13}$$

where ρ (9.87 g/cm^3) is a density of the thorium dioxide, whose molecular weight is A(264), N_0(6.02×10^{23}) is Avogadro's number and λ(0.495×10^{-10}/year) is a decay constant of ^{232}Th.

Two examples for the dosage and the self-absorption are shown in Figs. 6 and 7 respectively. One is in a case of radioactive equilibrium $p_1=p_2=\cdots p_7=1$, and the other in a case of a state of $p_1=1$, $p_2=0.5$, and $p_3=\cdots p_7=0.4$, which closely resemble the steady state equilibrium in tissue observed by some resear-

Table 2. The geometrical factor ($G\times10^4$) for the spherical aggregate of thorium dioxide as a function of α.

α \ δ	0	0.01	0.02	0.04	0.06	0.08	0.10	0.15	0.2	0.3	0.4	0.5	0.6	0.7	0.8	0.9
0.0010	13															
0.0016	21															
0.0025	33	1														
0.0040	52	3	1													
0.0063	83	8	3	1												
0.010	130	23	10	3	2	1	1									
0.016	208	57	29	12	6	4	3	1	1							
0.025	325	125	72	33	19	12	9	4	3	1	1					
0.040	520	263	171	92	57	39	29	16	10	5	3	2	1	1	1	
0.063	819	503	364	223	152	110	84	49	32	17	10	7	5	4	2	1
0.10	1300	922	729	501	371	287	229	143	99	55	35	24	16	10	5	2
0.16	2080	1639	1384	1052	837	685	573	392	285	165	101	63	38	22	11	3
0.25	3077	2578	2265	1824	1514	1280	1096	777	577	331	200	123	74	41	19	5
0.40	3798	3286	2955	2472	2116	1837	1610	1193	908	551	343	213	128	69	30	7
0.63	4237	3738	3416	2937	2576	2284	2042	1576	1240	791	509	321	191	101	42	10
1.0	4519	4046	3742	3287	2936	2649	2404	1918	1552	1030	679	431	255	134	56	13
1.6	4700	4256	3973	3547	3214	2935	2694	2202	1816	1238	826	527	313	164	69	16
2.5	4808	4392	4129	3728	3410	3140	2902	2407	2006	1385	932	599	358	189	79	19
4.0	4880	4492	4247	3868	3561	3297	3061	2558	2143	1493	1012	655	394	209	88	21
6.3	4924	4560	4329	3965	3664	3401	3164	2654	2231	1563	1065	693	418	223	94	23
10	4952	4610	4389	4033	3735	3471	3232	2717	2289	1610	1102	719	435	233	99	23
16	4970	4646	4431	4078	3780	3515	3275	2758	2326	1641	1126	737	447	240	102	24
25	4981	4671	4459	4109	3807	3542	3302	2783	2349	1660	1141	747	454	244	104	25
40	4988	4689	4478	4125	3826	3560	3319	2799	2365	1673	1151	755	459	247	105	25
63	4992	4700	4489	4137	3837	3571	3330	2810	2374	1680	1157	759	462	248	106	26
∞	5000	4720	4509	4156	3856	3590	3349	2827	2391	1694	1167	767	468	252	107	26

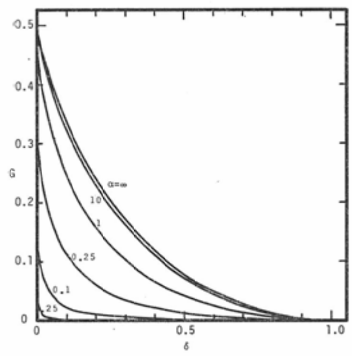

Fig. 4. The geometrical factor for the spherical aggregate of thorium dioxide as a function of α.

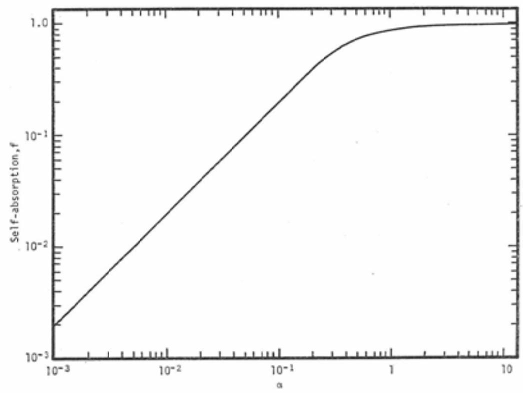

Fig. 5. The self-absorption as a function of α.

chers[14)15)16)17)]. The dose-rate at the surface of an aggregate was about 10 times higher even for 1μ of radius, and thousands times higher for 100μ of radius than the average dose-rate in the liver and the

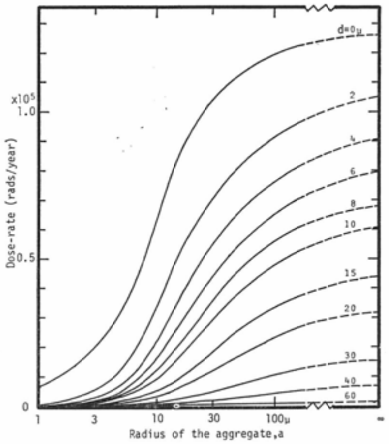

(a)

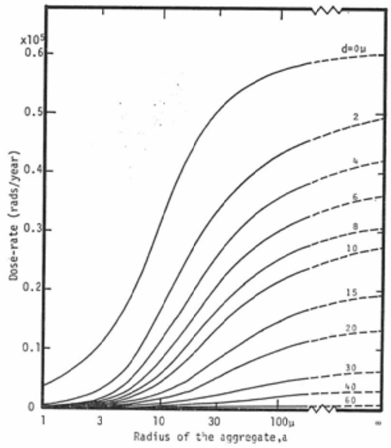

(b)

Fig. 6. The dose-rate as functions of d and a.

(a): the dose-rate in radioactive equilibrium ($p_1=p_2=\cdots=p_7=1$),

(b): the dose-rate in steady state equilibrium ($p_1=1$, $p_2=0.5$, $p_3=\cdots=p_7=0.4$).

spleen. In the self-absorption, it was also seen that the self-absorption was an important factor in estimating the total energy dissipated in tissue, when the radius of an aggregate was over 1μ.

If the mean self-absorption is used, an average dose-rate, $\bar{D}$, in tissue within a maximum range of the α-particles from a surface of an aggregate is easily estimated as follows:

$$\bar{D}=\frac{\frac{4}{3}\pi a^3 N\cdot\sum_i p_i E_i(1-f_i)}{\frac{4}{3}\pi\{(a+88.6)^3-a^3\}}=\frac{0.178\times10^5(1-\bar{f})\cdot\sum_i p_i E_i(\mathrm{MeV})}{(1+\frac{88.6}{a})^3-1} \quad \text{in rad/year.} \qquad (14)$$

The values of $\bar{D}$ for the two cases mentioned above were plotted in Fig. 8.

Estimations of average dose-rate and average self-absorption in some histological sections

Histological sections were taken from samples of the liver and the spleen of four thorotrast patients whose pathological findings and the average dose-rate in the organs were reported in our previous paper[6)]. The estimations were made for fibrous tissue areas, where the aggregates are distributed densely, and for non-fibrous tissue areas, where the aggregates with relatively small size are distributed diffusely. Frequency distributions* of the aggregate radius in the sections of 6μ in thickness are obtained from a view field with 450μ in diameter by using a microscope with a magnification of 400. Table 3 shows an example of the frequency distribution in the non-fibrous tissue areas. An apparent frequency of each range of the aggregate radius, n_{obs}, shown in second column, was an average value for 20 view fields selected in four sections. A true value, n_{tr}, of the frequency shown in fourth column was obtained by multiplying the

*: These frequency distributions of the aggregate radius in the histological sections of four thorotrast patients were provided by Dr. T. Mori in Department of Pathology, Yokohama University School of Medicine.

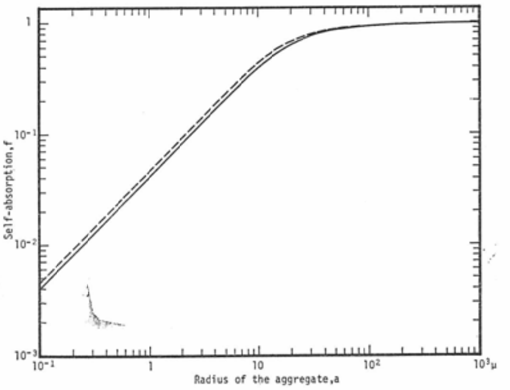

Fig. 7. The self-absorption of the aggregate as a function of a. Solid line: the self-absorption in radioactive equilibrium ($p_1=p_2=\cdots=p_7=1$). Broken line: the self-absorption in steady state equilibrium ($p_1=1$, $p_2=0.5$, $p_3=\cdots=p_7=0.4$).

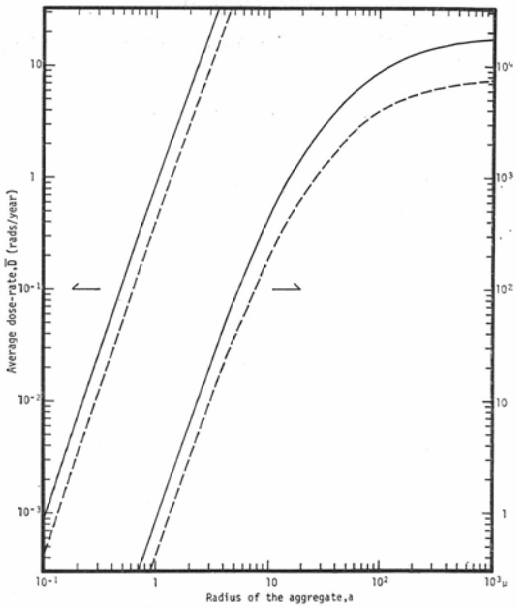

Fig. 8. The average dose-rate, $\overline{D}$, in tissue within a maximum range of α-particles from the aggregate surface.

Table 3. The frevuency distribution of the aggregate radius in the non-fibrous tissue area of the liver of case no. 896. The value of the frequency is an average value for 20 view fields selected in four sections.

Radius (a)	Apparent frequency (n_{obs})	Correction factor (g)	True frequency (n_{tr})	$n_{tr}a^3$	$\bar{f}$
0.5	7.05	0.853	6.01	0.8	0.023
1.75	7.60	0.622	4.73	25.3	0.080
3.75	3.60	0.430	1.55	81.6	0.171
7.5	0.45	0.268	0.121	50.9	0.336
12.5	0.05	0.174	0.00870	17.0	0.510

$\sum n_{tr}a^3 = 175.6$, $\sum \bar{f} n_{tr}a^3 = 41.8$, $\sum(1-\bar{f})n_{tr}a^3 = 133.8$,
F $=41.8/\ 175.6= 0.238$, D $=1.35\times 133.8= 181$=rads/year= 3.5 rads/week.

apparent value by a correction factor, g, which is roughly $1/\ (1+2a/h)\ (1+2a/d)^{2*)}$, where h is a thickness of the section and d is a diameter of the view field.

The average dose-rate and the average self-absorption in the section are given by

$$D_{tissue} = \frac{N(\sum_i p_i E_i)\frac{4}{3}\pi \cdot \sum_k n_k a_k^3 (1-\overline{f}_k)}{\pi(\frac{d}{2})^2 h} = 1.35 \cdot \sum_k n_k a_k^3 (1-\overline{f}_k), \quad (15)$$

and

$$F_{tissue} = \frac{\sum_k n_k a_k^3 \overline{f}_k}{\sum_k n_k a_k^3}. \quad (16)$$

The results are shown in Table 4, being compared with those of Rotblat et al.[3] who have estimated the average dose-rate and the average self-absorption in some histological sections by using the technique of α-track autoradiography. The values for non-fibrous tissue areas in the liver and the spleen accorded roughly with those of Rotblat et al. The values for fibrious tissue areas were considerably higher than those for non-fibrous tissue areas. The values of the self-absorption for the liver accorded roughly with those of Rotblat et al., but for the spleen were somewhat lower than theirs.

Table 4. The average dose-rate and the average self-absorption (in parentheses) in the non-fibrous tissue area and in the fibrous tissue area.

Case number	Liver		Spleen	
	Non-fibrous area	Fibrous area	Non-fibrous area	Fibrous area
	in rads/week			
896 (75cc inj.)	3.5 (0.24)	146 (0.61)	....	75 (0.68)
1200 (75cc inj.)	3.8 (0.22)	130 (0.52)	....	117 (0.59)
1243 (75cc inj.)	3.9 (0.55)	271 (0.53)	17 (0.48)	....
1520 (10cc inj.)	0.2 (0.09)	50 (0.42)	0.6 (0.23)	116 (0.45)
Rotblt et al.[3] Autoradigraphic measurement (22cc inj.)	8.1 (0.44)		Hilum ; 3.5 (0.71) Interior portion ; 4.8 (0.98) Exterior portion ; 8.3 (0.73)	

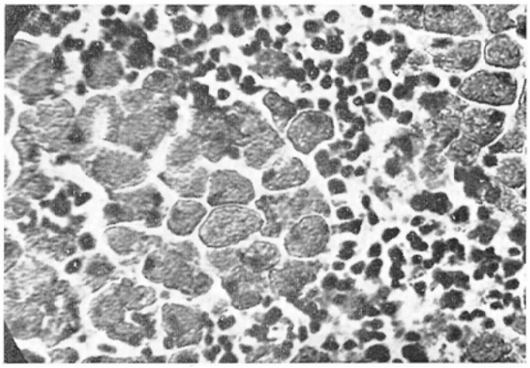

Fig. 9. A microscopic view of the spleen tissue of a mouse taken at six months after injection of thorotrast (2.5 ml/kg). A large thorotrast aggregate (about 80 μ in diameter) at the left portion of the picture is made of smaller thorotrast aggregates (about 15 μ in diameter) and inter-aggregate substances consist of cell elements and fibrous tissues. ×400.

*: If the rough estimation stands that a radius of any section made by a plane cutting a sphere with a radius of a is equal to the radius of this sphere, this expression turns to the following: Since, when a center of a sphere with a radius of a is persent within a distance of a from both surfaces of a histological section with a thickness of h, a part of this sphere are found in this section, a number of the spheres with the radius of a in that section may be over-estimated by (h+2a)/h. Then this number should be corrected by a factor of 1+2a/h for obtaining a true number. Similarly, a correction factor for a circumference of a view field is obtained to be $\left(\frac{d+2a}{d}\right)^2$. Therefore, the total correction factor, g, for the apparent value becomes $1/\left(1+\frac{2a}{h}\right)\left(1+\frac{2a}{d}\right)^2$.

In calculating the dosage and the self-absorption, it was assumed that the aggregate consists of thorium dioxide alone. But, in fact, the aggregate is a cluster of the granules of thorium dioxide with a diameter of 30 to 100Å[18] and cavities in the cluster are filled up with a number of small unknown fragments. Furthermore, the large aggregate with a diameter over 30μ is made of the smaller aggregates and inter-aggregate substances consists of cell elements and fibrous tissues as shown in Fig. 9. Therefore, the values of N and n for the thorotrast aggregate may become smaller than those used in this paper, and the actual values of the dosage and the self-absorption may be somewhat smaller than those estimated. The dose-rate in the inter-aggregate substances may be fairly high as compared with that outside of the aggregate.

Summary

The absorbed dose-rate due to α-particles near the thorotrast aggregate was estimated. The dose-rate at the surface of the aggregate was about 10^4 rad/year for the aggregate with a diameter over 10μ. The α-particle self-absorption in the aggregate was also estimated, and this value was applied to the estimation of the average absorbed dose-rate in some histological sections of the liver and the spleen. The average dose-rate in the fibrous tissue was considerably higher than that in the non-fibrous tissue in the liver and the spleen.

Acknowledgement

The author wishes to thank Dr. T. Hashizume for many helpful discussions and suggestions made during this work and Dr. T. Mori for providing the frequency distributions of the aggregate radius in the histological sections. The author is also grateful to Dr. S. Maruyama for valuable advices and comments in preparing this manuscript.

References

1) Hursh, J.B., Steadman, L.T., Looney, W.B., and Colodzin, M., 1957, Acta Radiol., 47, 481—498.
2) Looney, W.B., 1960, Am. J. Roentgenol. & Rad. Therapy, 83, 163—185.
3) Rotblat, J. and Ward, G.B., 1953, Nature, 172, 769—770.
4) Rundo, J., 1955, Brit, J, Radiol., 28, 615—619.
5) Schulz, R.J., 1958, Radiology, 70, 94—95.
6) Tsuya, A., Tanaka, T., Mori, T., Hashizume, T., and Kato, Y., 1963, J. Rad. Res., 4, 126—145.
7) Kaul, A., 1964, Assessment of Radioactivity in Man, Vol, 2, 445—471, International Atomic Energy Agency, Vienna.
8) Cohn, S.H., Gusmano, E.A., and Robertson, J.S., 1965, Meeting on Dosimetry and Toxicity of Thorotrast, International Atomic Energy Agency, Vienna, 4—7, Oct., 1965.
9) Spiers, F.W., 1949, Brit. J. Radiol., 22, 521—533.
10) Spiers, F.W., 1953, Brit. J. Radiol., 26, 296—301.
11) Strominger, D., Hollander, J.M., and Seaborg, G.T., 1958, Revs. Mod. Phys., 30, 585—904.
12) Whaling, W., 1958, Handbuch der Physik, 34, 193—217.
13) Evans, R.D., 1955, The Atomic Nucleus, p. 652, McGraw-Hill, New York.
14) Rundo, J., 1956, Phys. Med. Biol., 1, 138—146.
15) Marinelli, L.D., and Lucas, H.F.Jr., 1962, Some Aspects of Internal Irradiation, p. 499, Pergamon Press, Oxford.
16) Kaul, A., 1965, Meeting on Dosimetry and Toxicity of Thorotrast, International Atomic Energy Agency, Vienna, 4—7, Oct., 1965.
17) Unnewehr, F., Kaul, A., and Stahlhofen, W., 1964, Atomkernenergie, 9, 181—185.
18) Okawara, S., 1966, Nippon Acta Radiologica, 25, 1182—1188.